Research Article

Chaotic Control and Generalized Synchronization for a Hyperchaotic Lorenz-Stenflo System

Yin Li,[1,2] Yulin Zhao,[1] and Zheng-an Yao[1]

[1] *Department of Mathematics and Computational Science, Sun Yat-Sen University, Guangzhou 510275, China*
[2] *School of Mathematics and Information Science, Shaoguan University, Shaoguan 512005, China*

Correspondence should be addressed to Yin Li; liyin2009521@163.com

This paper is devoted to investigate the tracking control and generalized synchronization of the hyperchaotic Lorenz-Stenflo system using the tracking model and the feedback control scheme. We suppress the chaos to unstable equilibrium via three feedback methods, and we achieve three globally generalized synchronization controls. Novel tracking controllers with corresponding parameter update laws are designed such that the Lorenz-Stenflo systems can be synchronized asymptotically. Moreover, numerical simulations are presented to demonstrate the effectiveness, through the contrast between the orbits before being stabilized and the ones after being stabilized.

1. Introduction

Study of chaotic control and generalized synchronization has received great attention in the past several decades [1–10]; many hyperchaotic systems have been proposed and studied in the last decade, for example, a new hyperchaotic Rössler system [4], the hyperchaotic L system [5], Chua's circuit [6], the hyperchaotic Chen system [7, 8], and so forth. Hyperchaotic system has been proposed for secure communication and the presence of more than one positive Lyapunov exponent clearly improves the security of the communication scheme [9–12]. Therefore, hyperchaotic system generates more complex dynamics than the low-dimensional chaotic system, which has much wider application than the low-dimensional chaotic system.

Until now, a variety of approaches have been proposed for the synchronization of low-dimensional chaotic systems, including Q-S method [13, 14], active control [15, 16], adaptive control [17–24], and time-delay feedback control [25]. Recently, Stenflo [26] presented a new hyperchaotic Lorenz-Stenflo (LS) system:

$$
\begin{aligned}
\dot{x} &= a\left(y - x\right) + dw, \\
\dot{y} &= x\left(c - z\right) - y, \\
\dot{z} &= yx - bz, \\
\dot{w} &= -x - aw.
\end{aligned}
\tag{1}
$$

In (1), x, y, z, and w are the state variables of the system and a, b, c, and d are real constant parameters. System (1) is generated from the originally three-dimensional Lorenz chaotic system by introducing a new control parameter b and a state variable w.

In this paper, we will consider chaos control and generalized synchronization related to hyperchaotic Lorenz-Stenflo system. we found that the feedback control achieved in the low-dimensional system like many other studies of dynamics in low-dimensional systems. We suppress the hyperchaotic Lorenz-Stenflo system to unstabilize equilibrium via three control methods: linear feedback control, speed feedback control, and doubly-periodic function feedback control. By designing a nonlinear controller, we achieve the generalized synchronization of two Lorenz-Stenflo systems up to a scaling factor. Moreover, numerical simulations are applied to verify the effectiveness of the obtained controllers.

2. The Hyperchaotic Lorenz-Stenflo System

In the following we would like to consider the hyperchaotic cases of system (1). When $a = 1.0$, $b = 0.7$, $c = 26$, and $d = 1.5$, system (1) exhibits hyperchaotic behavior. Simulated results are depicted in Figures 1 and 2. Figures 1(a)–1(d) depict the projection of the chaotic attractor in different spaces; Figures 2(a)–2(d) depict the states of system (1) before being
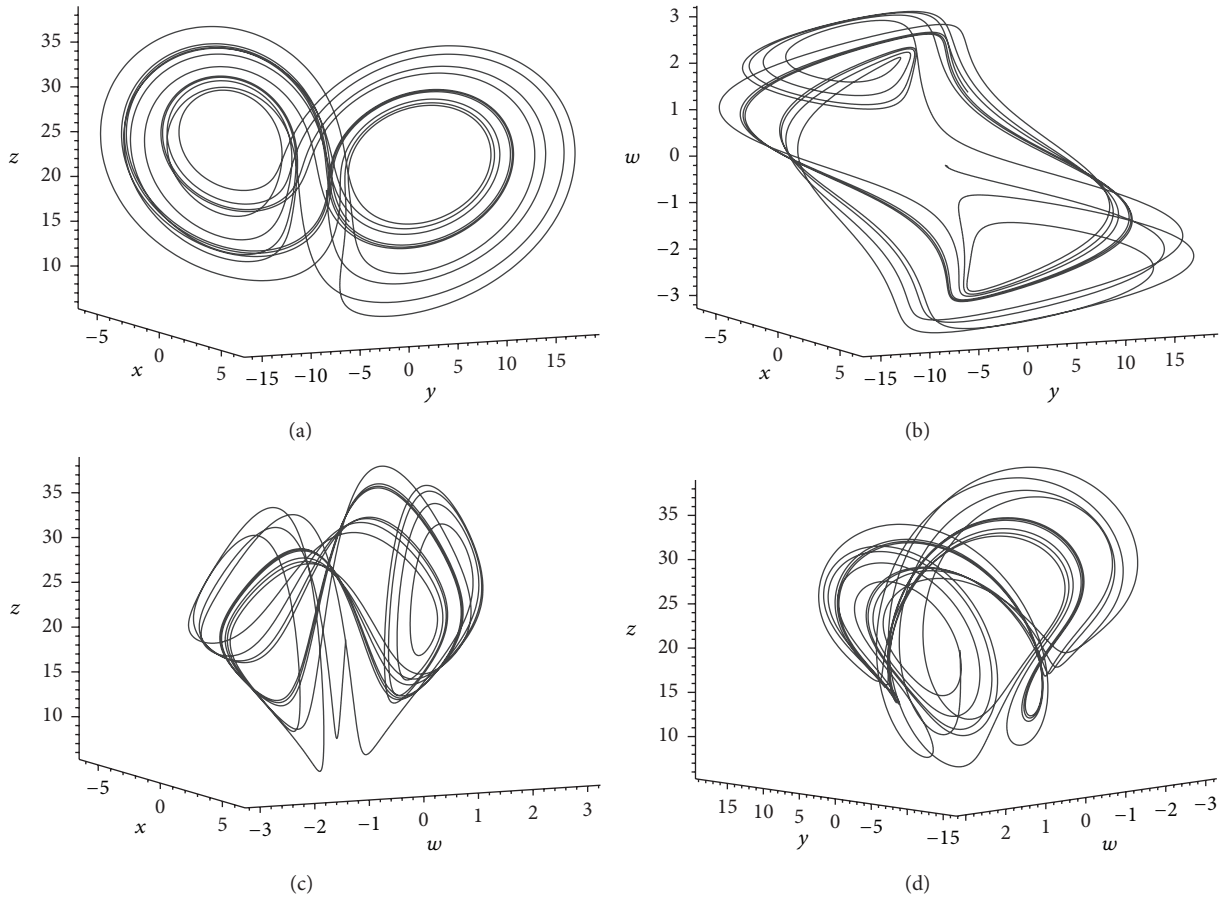
Figure 1: Chaotic attractor in different spaces: (a) (x, y, z), (b) (x, y, w), (c) (x, w, z), and (d) (y, w, z).

stabilized, respectively. The volume of the elements in the phase space $\delta X(t) = \delta x \delta y \delta z \delta w$ and the divergence of flow (1) are defined by

$$\nabla X = \frac{\partial X}{\partial x} + \frac{\partial X}{\partial y} + \frac{\partial X}{\partial z} + \frac{\partial X}{\partial w} = -(2a + b + 1), \quad (2)$$

where $X = (\dot{x}, \dot{y}, \dot{z}, \dot{w}) = [a(y - x) + dw, x(c - z) - y, yx - bz, -x - aw]$.

System (1) is dissipative when $2a + b + 1 > 0$. Moreover, an exponential contraction rate is given by

$$\frac{dX(t)}{dt} = -(2a + b + 1) X(t). \quad (3)$$

It is clear that $X(t) = X_0 e^{-(2a+b+1)t}$, which implies that the solutions of system (1) are bounded as $t- > +\infty$. It is easy to find the three equilibria $E_1(0, 0, 0, 0)$,

$$E_2\left(\frac{\sqrt{((c-1)a^2 - d)b(d + a^2)}}{d + a^2}, \right.$$

$$\frac{\sqrt{((c-1)a^2 - d)b(d + a^2)}}{a^2},$$

$$\frac{(c-1)a^2 - d}{a^2},$$

$$\left. -\frac{\sqrt{(d + a^2)b(a^2c - a^2 - d)}}{(d + a^2)a} \right),$$

$$E_3\left(-\frac{\sqrt{((c-1)a^2 - d)b(d + a^2)}}{d + a^2}, \right.$$

$$-\frac{\sqrt{((c-1)a^2 - d)b(d + a^2)}}{a^2},$$

$$\left. \frac{(c-1)a^2 - d}{a^2}, \frac{\sqrt{(d + a^2)b(a^2c - a^2 - d)}}{(d + a^2)a} \right).$$

$$(4)$$

To determine the stability of the equilibria point $E_1(0, 0, 0, 0)$, evaluating the Jacobian matrix of system (1) at E_1 yields

$$J|_{E_1} = \begin{pmatrix} -a & a & 0 & d \\ c & -1 & 0 & 0 \\ 0 & 0 & -b & 0 \\ -1 & 0 & 0 & -a \end{pmatrix}. \quad (5)$$
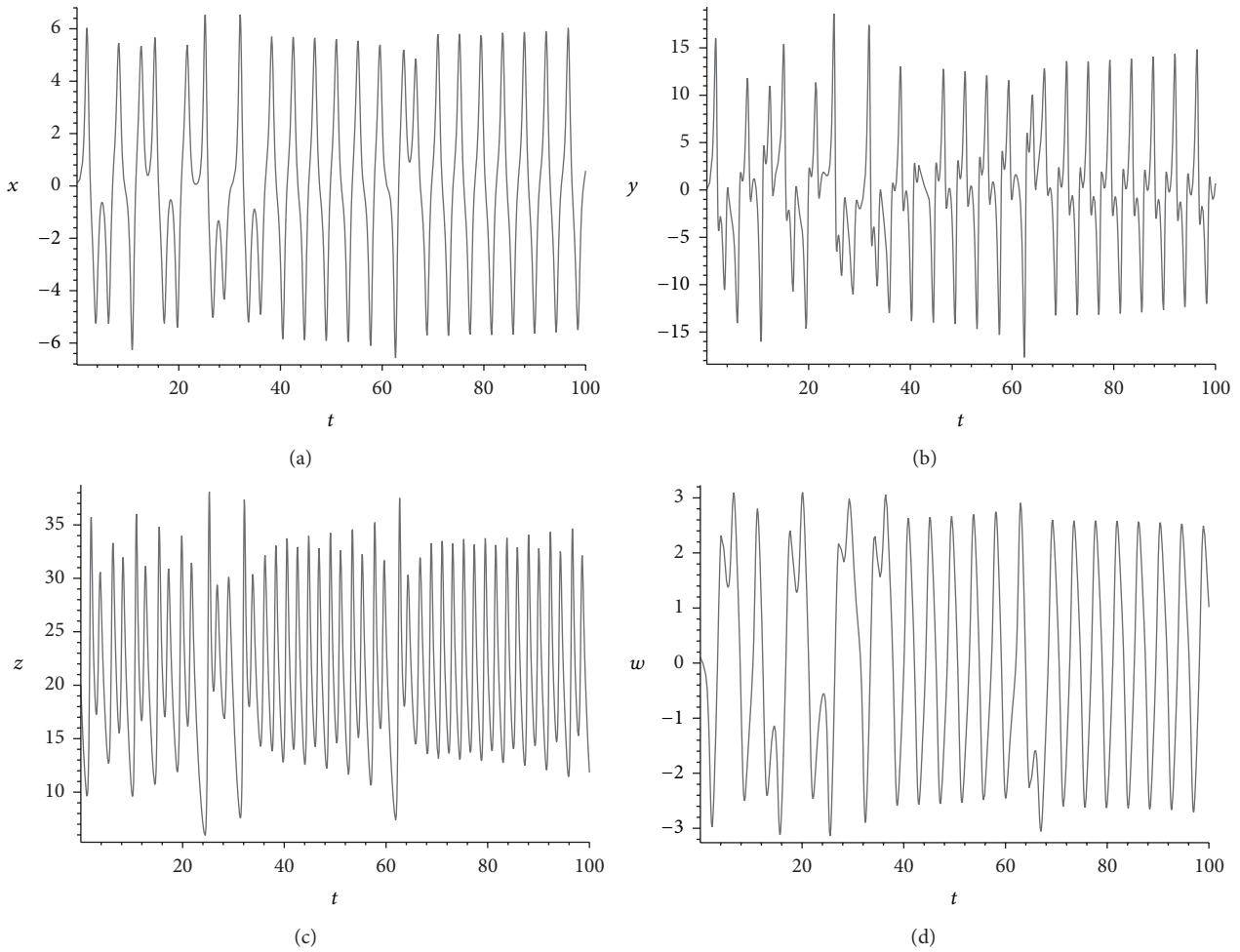
Figure 2: The states of system (1) before being stabilized: (a) x-t, (b) y-t, (c) z-t, and (d) w-t.

If $a = 1.0$, $b = 0.7$, $c = 26$, and $d = 1.5$, the four eigenvalues of the characteristic polynomial of Jacobian matrix (5) are

$$\lambda_1 = 3.94975, \quad \lambda_2 = -5.9497, \quad \lambda_3 = -1, \quad \lambda_4 = -0.7. \tag{6}$$

Thus, the equilibria E_1 is a saddle point of the hyperchaotic system (1). The Jacobian matrix of system (1) at E_2 yields

$$J|_{E_2} = \begin{pmatrix} -a & a & 0 & d \\ c & -1 & \dfrac{\sqrt{((c-1)a^2 - d)b(d + a^2)}}{d + a^2} & 0 \\ \dfrac{\sqrt{((c-1)a^2 - d)b(d + a^2)}}{a^2} & \dfrac{\sqrt{((c-1)a^2 - d)b(d + a^2)}}{d + a^2} & -b & 0 \\ -1 & 0 & 0 & -a \end{pmatrix}. \tag{7}$$

If $a = 1.0$, $b = 0.7$, $c = 26$, and $d = 1.5$, the four eigenvalues of the characteristic polynomial of Jacobian matrix (7) are

$$\lambda_1 = 4.8887, \quad \lambda_2 = -6.3032,$$

$$\lambda_3 = -1.1427 + 0.5438i, \quad \lambda_4 = -1.1427 - 0.5438i. \tag{8}$$

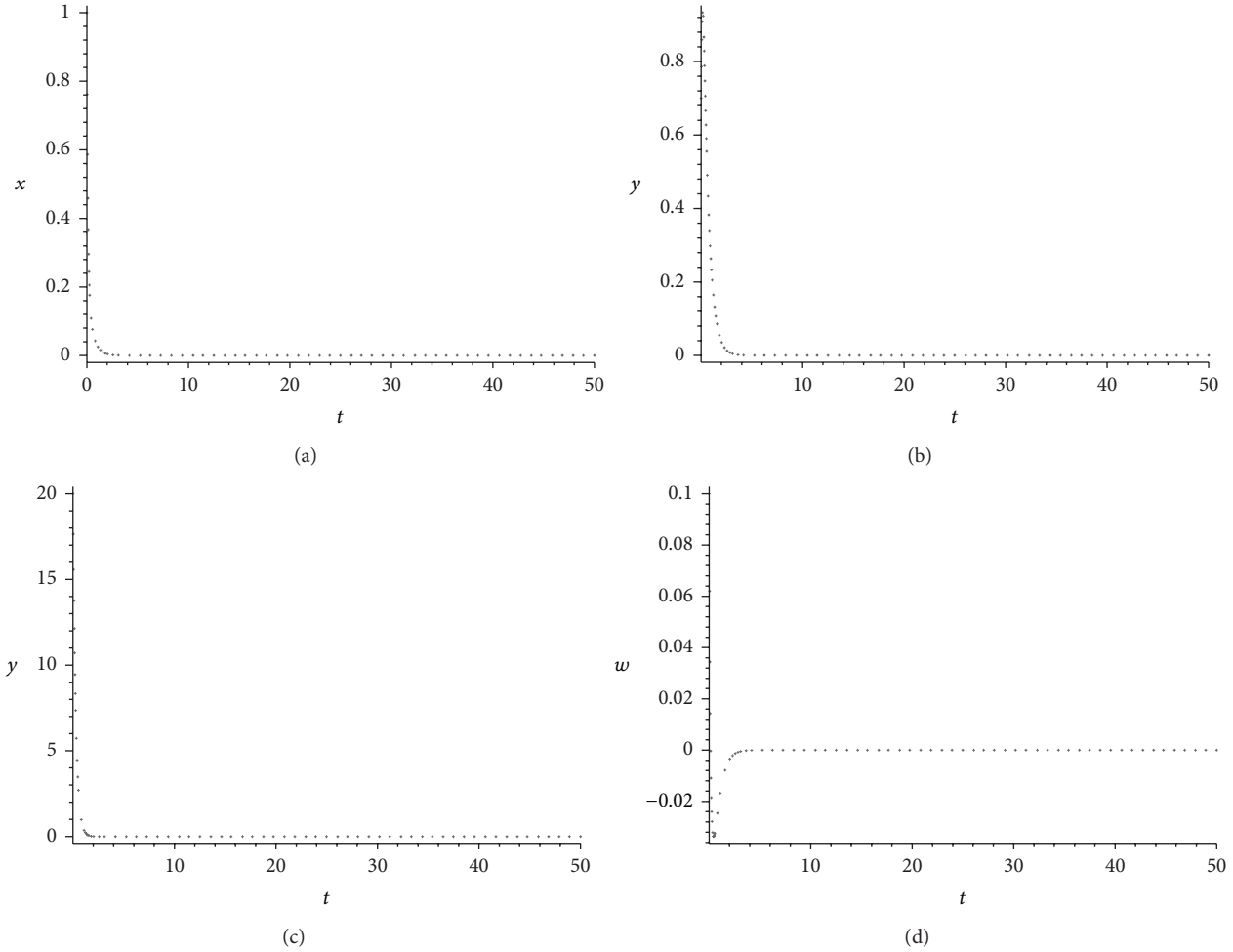Thus, the equilibria E_2 are unstable, and E_3 is similar.

Figure 3: The states of system (9): (a) x-t, (b) y-t, (c) z-t, (d) w-t.

3. The Hyperchaotic Control for Lorenz-Stenflo System

In this section, we control the hyperchaotic system (1) such that all trajectories converge to the equilibrium point $(0, 0, 0, 0)$. The controlled hyperchaotic Lorenz-Stenflo system is given by

$$
\begin{aligned}
\dot{x} &= a(y - x) + dw + u_1, \\
\dot{y} &= x(c - z) - y + u_2, \\
\dot{z} &= yx - bz + u_3, \\
\dot{w} &= -x - aw + u_4,
\end{aligned}
\tag{9}
$$

where u_1, u_2, u_3, and u_4 are external control inputs which will be suitably derived from the trajectory of the chaotic system (1), specified by (x, y, z, w) to the equilibrium $(0, 0, 0)$ of uncontrolled system $u_i = 0$ $(i = 1, 2, 3, 4)$.

3.1. Linear Function Feedback Control. For the modified hyperchaotic Lorenz-Stenflo system (9), if one of the following feedback controllers u_i $(i = 1, 2, 3, 4)$ is chosen for the

system (9), then $u_1 = -k_1 x_1$, $u_2 = -k_2 y$, $u_3 = -k_3 z$, $u_4 = -k_4 w$, and where k_i's are feedback coefficients. Therefore controlled system (9) is rewritten as

$$
\begin{aligned}
\dot{x} &= a(y - x) + dw - k_1 x, \\
\dot{y} &= x(c - z) - y - k_2 y, \\
\dot{z} &= yx - bz - k_3 z, \\
\dot{w} &= -x - aw - k_4 w
\end{aligned}
\tag{10}
$$

whose Jacobian matrix is

$$
J = \begin{pmatrix}
-a - k_1 & a & 0 & d \\
c & -1 - k_2 & 0 & 0 \\
0 & 0 & -b - k_3 & 0 \\
-1 & 0 & 0 & -a - k_4
\end{pmatrix}.
\tag{11}
$$

The characteristic equation of J is

$$
\lambda^4 + (-B - A - D - C)\lambda^3
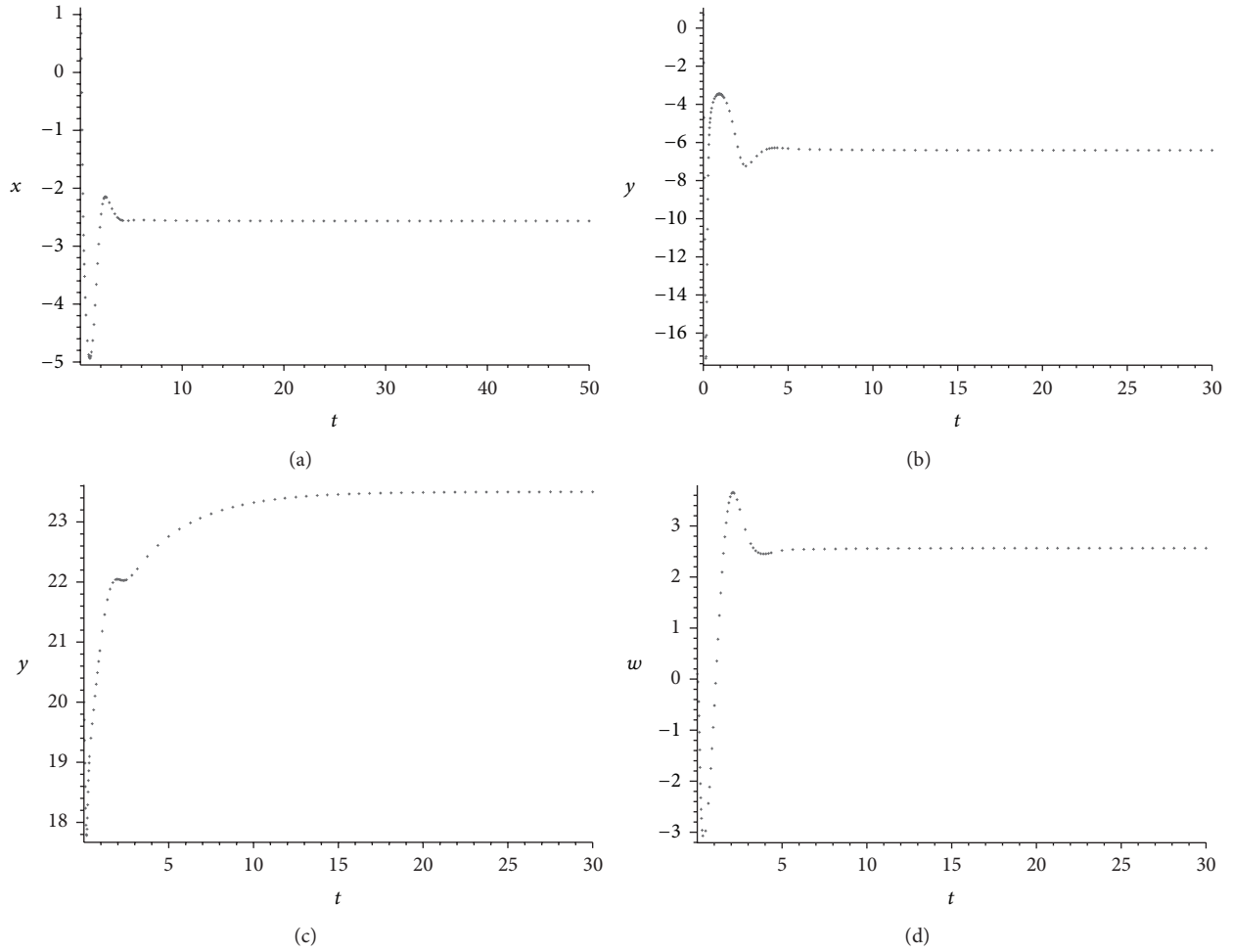$$
$$
+ (CD + AB + BD + BC - ca + AD + AC + d)\lambda^2
$$

FIGURE 4: The states of system (19): (a) x-t, (b) y-t, (c) z-t, and (d) w-t.

$$+ (-ABD - ABC - BCD + caD$$
$$+ caC - ACD - dC - dB) \lambda + E = 0,$$

(12)

where $A = -a - k_1$, $B = -1 - k_2$, $C = -b - k_3$, $D = -a - k_4$, and $E = ABCD - caCD + dBC$.

The abbreviated characteristic equation is

$$\lambda^4 + R_1 \lambda^3 + R_2 \lambda^2 + R_3 \lambda + E = 0, \quad (13)$$

where $R_1 = -B - A - D - C$, $R_2 = CD + AB + BD + BC - ca + AD + AC + d$, and $R_3 = -ABD - ABC - BCD + caD + caC - ACD - dC - dB$, $R_4 = E$.

According to the Routh-Hurwitz criterion, constraints are imposed as follows:

$$H_1 = R_1 = -B - A - D - C > 0,$$

$$H_2 = \begin{vmatrix} R_1 & R_3 \\ 1 & R_2 \end{vmatrix} = R_1 R_2 - R_3$$

$$= (-A - C - B) D^2$$

$$+ \left((-2A - 2C) B - B^2 - A^2 - C^2 - d - 2AC \right) D$$

$$+ (-A - C) B^2 - A^2 C + \left(-2AC + ca - A^2 - C^2 \right) B$$

$$+ \left(-d - C^2 + ca \right) A > 0,$$

$$H_3 = \begin{vmatrix} R_1 & R_3 & 0 \\ 1 & R_2 & E \\ 0 & R_1 & R_3 \end{vmatrix} = R_1 R_2 R_3 - E R_1^2 - R_3^2 > 0,$$

$$H_4 = \begin{vmatrix} R_1 & R_3 & 0 & 0 \\ 1 & R_2 & R_4 & 0 \\ 0 & R_1 & R_3 & 0 \\ 0 & 1 & R_2 & R_4 \end{vmatrix}$$

$$= R_1 R_2 R_3 R_4 - R_1^2 R_4^2 - R_3^2 R_4 > 0.$$

(14)

This characteristic polynomial has four roots, all with negative real roots, under the condition of $H_1 > 0$, $H_2 > 0$, $H_3 > 0$, and $H_4 > 0$. Therefore, the equilibria $(0,0,0,0)$ are the stable manifold W^s and the controlled chaotic Lorenz-Stenflo system (9) is asymptotically stable. The concrete dynamics of
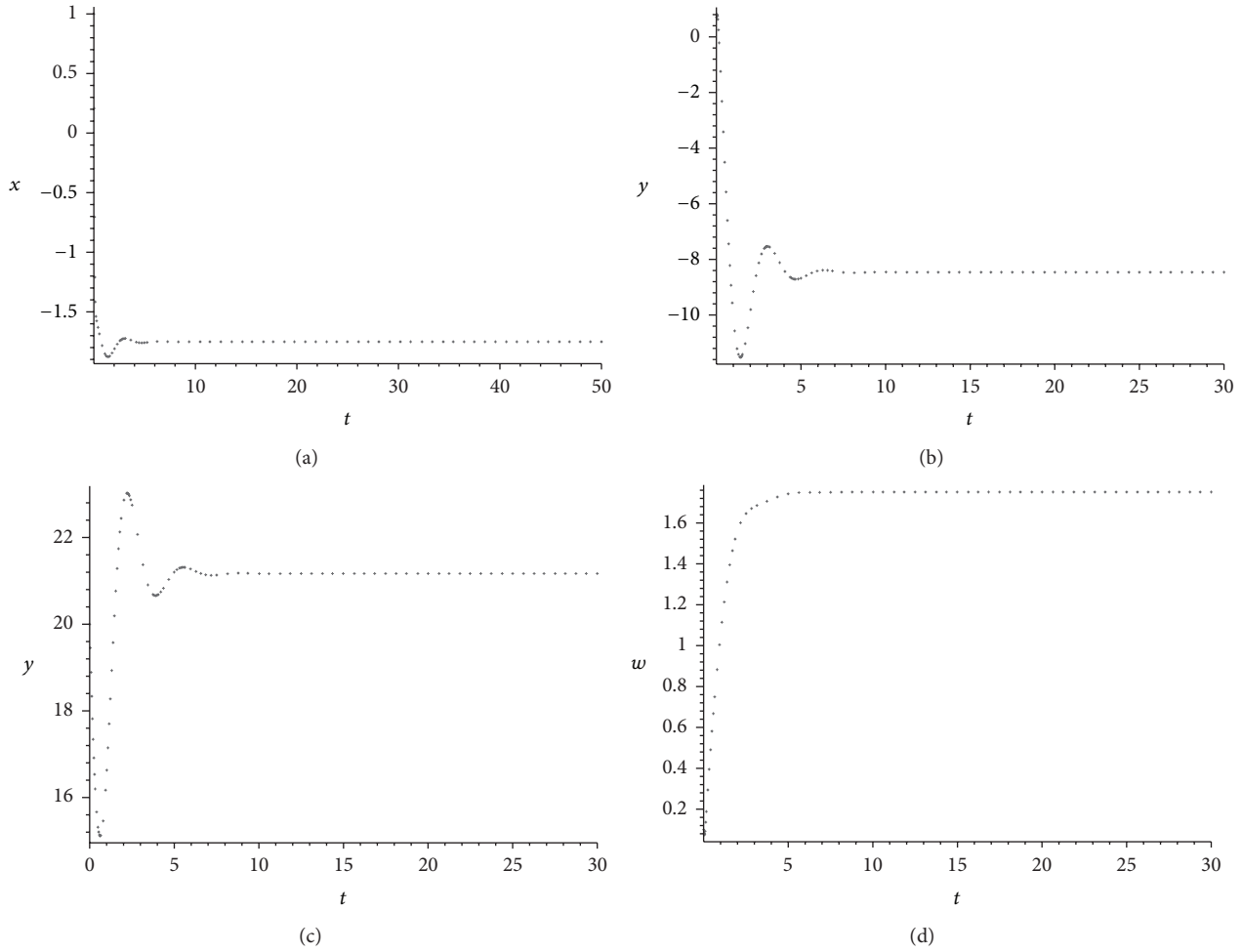
FIGURE 5: The states of system (25): (a) x-t, (b) y-t, (c) z-t, and (d) w-t.

(9) can be demonstrated by Proposition 1, while the Maple program is demonstrated in Appendix A.

Proposition 1. *If one chooses the control coefficients $k_1 = 8$, $k_2 = 4$, $k_3 = 3$, and $k_4 = 2$ and the parameters $a = 1.0$, $b = 0.7$, $c = 26$, and $d = 1.5$, the controlled chaotic Lorenz-Stenflo system* (9) *is asymptotically stable at the equilibrium* $(0, 0, 0, 0)$.

Proof. When the parameters were selected by the above value, we obtain the Jacobian matrix

$$J = \begin{pmatrix} -9.0 & 1.0 & 0 & 1.5 \\ 26 & -5 & 0 & 0 \\ 0 & 0 & -3.7 & 0 \\ -1 & 0 & 0 & -3.0 \end{pmatrix}. \qquad (15)$$

The characteristic equation of J is given by

$$\lambda^4 + 20\frac{7}{10}\lambda^3 + 125\frac{2}{5}\lambda^2 + 295\frac{3}{4}\lambda + 238\frac{13}{20} = 0. \qquad (16)$$

According to Appendix A, we easily obtain

$$H_1 = 20\frac{7}{10} > 0, \qquad H_2 = 2300 > 0,$$
$$\qquad (17)$$
$$H_3 = 578 > 0, \qquad H_4 = \frac{69}{500} > 0,$$

which yields the eigenvalues via the compute simulation

$$\lambda_1 = -12.36844706, \quad \lambda_2 = -1.931149367,$$
$$\qquad (18)$$
$$\lambda_3 = -2.700403573, \quad \lambda_4 = -3.70000.$$

Thus the zero solution of system (9) is exponentially stable, Proposition 1 is proved. $\qquad \square$

Numerical simulations are used to investigate the controlled chaotic Lorenz-Stenflo system (1) using the fourth-order Runge-Kutta scheme with time step 0.01. The parameters and the corresponding feedback coefficients are given by the above value. The initial values are taken as $[x(0) = 1, y(0) = 0.7, z(0) = 20, w(0) = 0.1]$. The behaviors of the states (x, y, z, w) of the controlled chaotic Lorenz-Stenflo system (1) with time are displayed in Figures 3(a)–3(d).
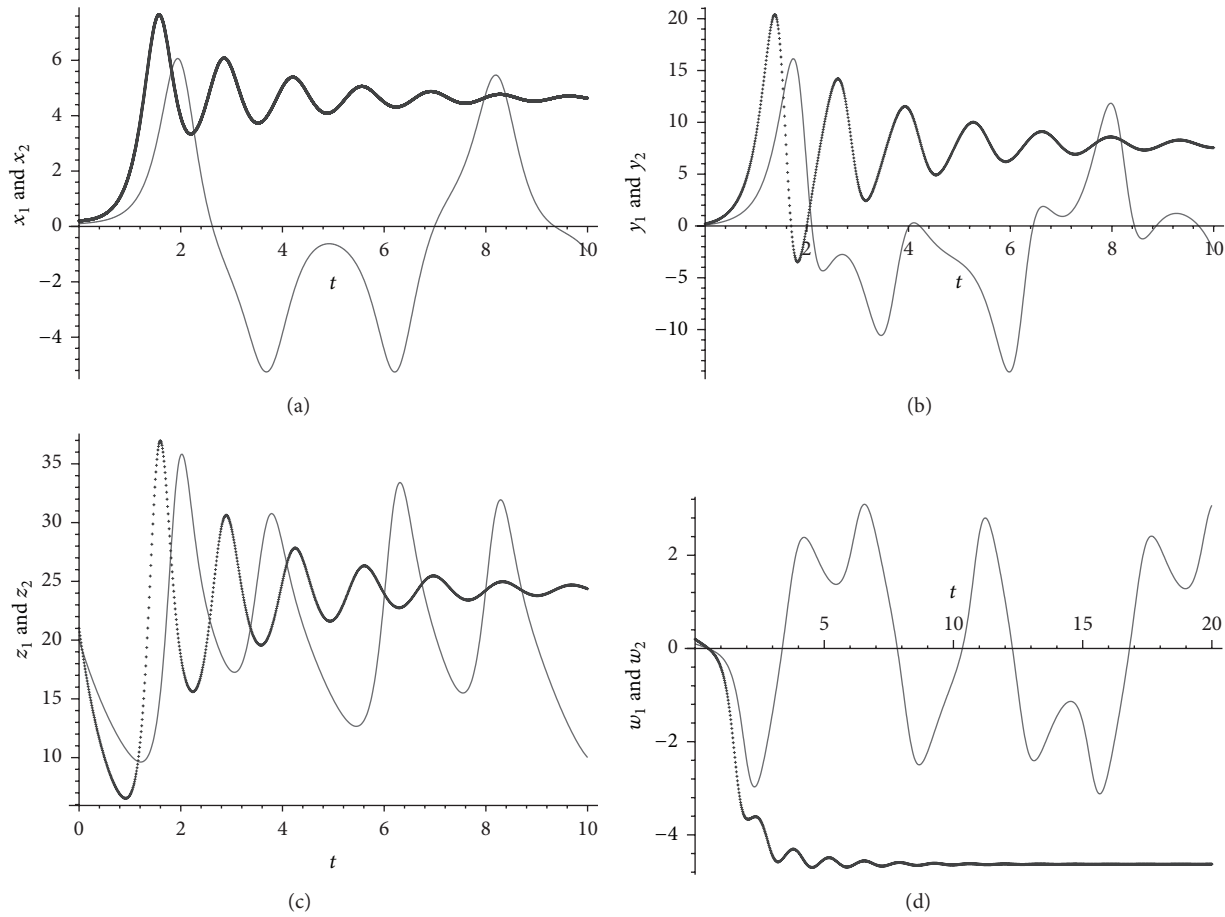
(a)

(b)

(c)

(d)

FIGURE 6: The solutions of the master and slave systems without active control law. (a) Signals x_1 (the dashed line) and x_2 (the solid line). (b) Signals y_1 (the dashed line) and y_2 (the solid line). (c) Signals z_1 (the dashed line) and z_2 (the solid line). (d) Signals w_1 (the dashed line) and w_2 (the solid line).

3.2. Speed Function Feedback Control. Suppose that $u_1 = u_3 = 0$; u_2 and u_4 are of the speed forms $u_2 = k_2(-bz + xy)$ and $u_4 = -k_4[a(y-x) + dw]$, where k_2 and k_4 are speed feedback coefficients. Therefore the controlled chaotic system (9) is rewritten as

$$\dot{x} = a(y - x) + dw,$$

$$\dot{y} = x(c - z) - y + k_2(-bz + xy),$$

$$\dot{z} = yx - bz, \tag{19}$$

$$\dot{w} = -x - aw - k_4[a(y - x) + dw].$$

The Jacobian matrix is

$$J = \begin{pmatrix} -a & a & 0 & d \\ c & -1 & -k_2 b & 0 \\ 0 & 0 & -b & 0 \\ -1 + k_4 a & -k_4 a & 0 & -a - k_4 d \end{pmatrix}. \tag{20}$$

The characteristic equation of J is

$$\lambda^4 + (1 - k_1 + 2a + b)\lambda^3$$

$$+ (2ab - k_1 b - k_1 a + 2a - k_1 + b + d + a^2 - ca)\lambda^2$$

$$+ (-ca^2 - cab + 2ab + db + a^2 b - k_1 a$$

$$+ a^2 - k_1 b - k_1 ba + d)\lambda$$

$$- ca^2 b - k_1 ba + a^2 b + db = 0. \tag{21}$$

Proposition 2. *If one chooses the control coefficients: $k_2 = 9$, $k_4 = -1$ and the parameters $a = 1.0$, $b = 0.7$, $c = 26$, and $d = 1.5$, the controlled chaotic Lorenz-Stenflo system (9) is asymptotically stable at the equilibrium $(0, 0, 0, 0)$.*

Similar to Proposition 1, the proof of Proposition 2 is straightforward and thus is omitted.

In the following, we give the eigenvalues via the compute simulation. When the parameters were selected by the above value, we obtain the Jacobian matrix

$$J = \begin{pmatrix} -1.0 & 1.0 & 0 & 1.5 \\ 26 & -1 & -6.3 & 0 \\ 0 & 0 & -0.7 & 0 \\ -2.0 & 1.0 & 0 & 0.5 \end{pmatrix}. \tag{22}$$
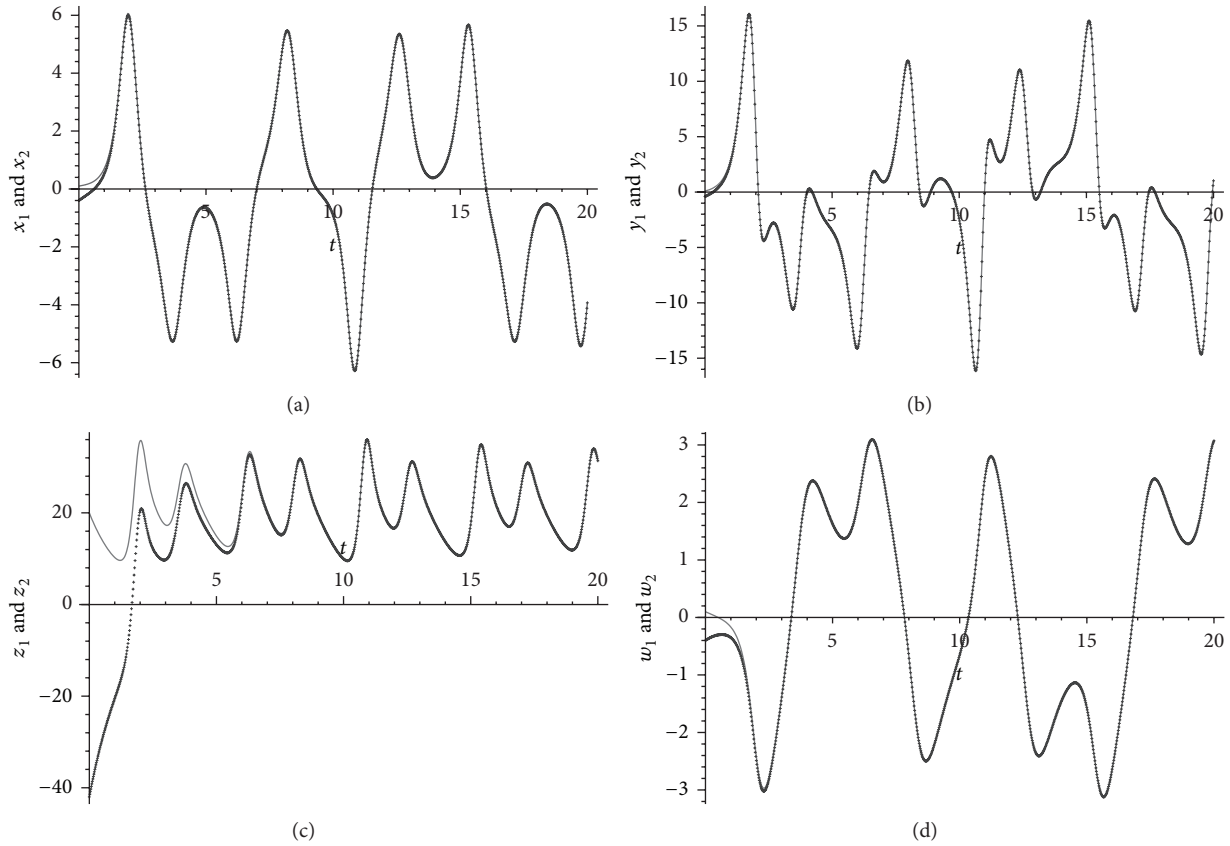
(a)

(b)

(c)

(d)

FIGURE 7: The solutions of the drive and response systems with control law. (a) Signals x_1 (the dashed line) and x_2 (the solid line). (b) Signals y_1 (the dashed line) and y_2 (the solid line). (c) Signals z_1 (the dashed line) and z_2 (the solid line). (d) Signals w_1 (the dashed line) and w_2 (the solid line).

The characteristic equation of J changes the following:

$$\lambda^4 + 2.2\lambda^3 - 21.95\lambda^2 - 39.6\lambda - 16.45 = 0. \qquad (23)$$

The eigenvalues of the above equation are

$$\lambda_1 = -5.10412, \quad \lambda_2 = -1,$$
$$\lambda_3 = -0.70000, \quad \lambda_4 = -4.60412. \qquad (24)$$

Numerical simulations are used to investigate the controlled chaotic Lorenz-Stenflo system (20) using the fourth-order Runge-Kutta scheme with time step 0.01. The initial values are taken as $[x(0) = 1, y(0) = 0.7, z(0) = 20, w(0) = 0.1]$. The behaviors of the states (x, y, z, w) of the controlled chaotic Lorenz-Stenflo system (20) with time are displayed in Figures 4(a)–4(d).

3.3. *The Doubly Periodic Function Feedback Control.* Suppose that $u_2 = 0$, $u_3 = 0$, and $u_4 = 0$; u_1 is of the doubly periodic function $u_1 = k_1 cn(x, m)$, where k_1 is speed feedback coefficients and $0 < m < 1$ is the modulus of Jacobi

elliptic function. Therefore the controlled chaotic system (9) is rewritten as

$$\dot{x} = a(y - x) + dw + k_1 cn(x, m),$$
$$\dot{y} = x(c - z) - y,$$
$$\dot{z} = yx - bz, \qquad (25)$$
$$\dot{w} = -x - aw.$$

The Jacobian matrix is

$$J = \begin{pmatrix} -a + k_1 & a & 0 & d \\ c & -1 & 0 & 0 \\ -1 & 0 & 0 & -a \end{pmatrix}. \qquad (26)$$

The characteristic equation of J is

$$\lambda^4 + (1 - k_1 + 2a + b)\lambda^3$$
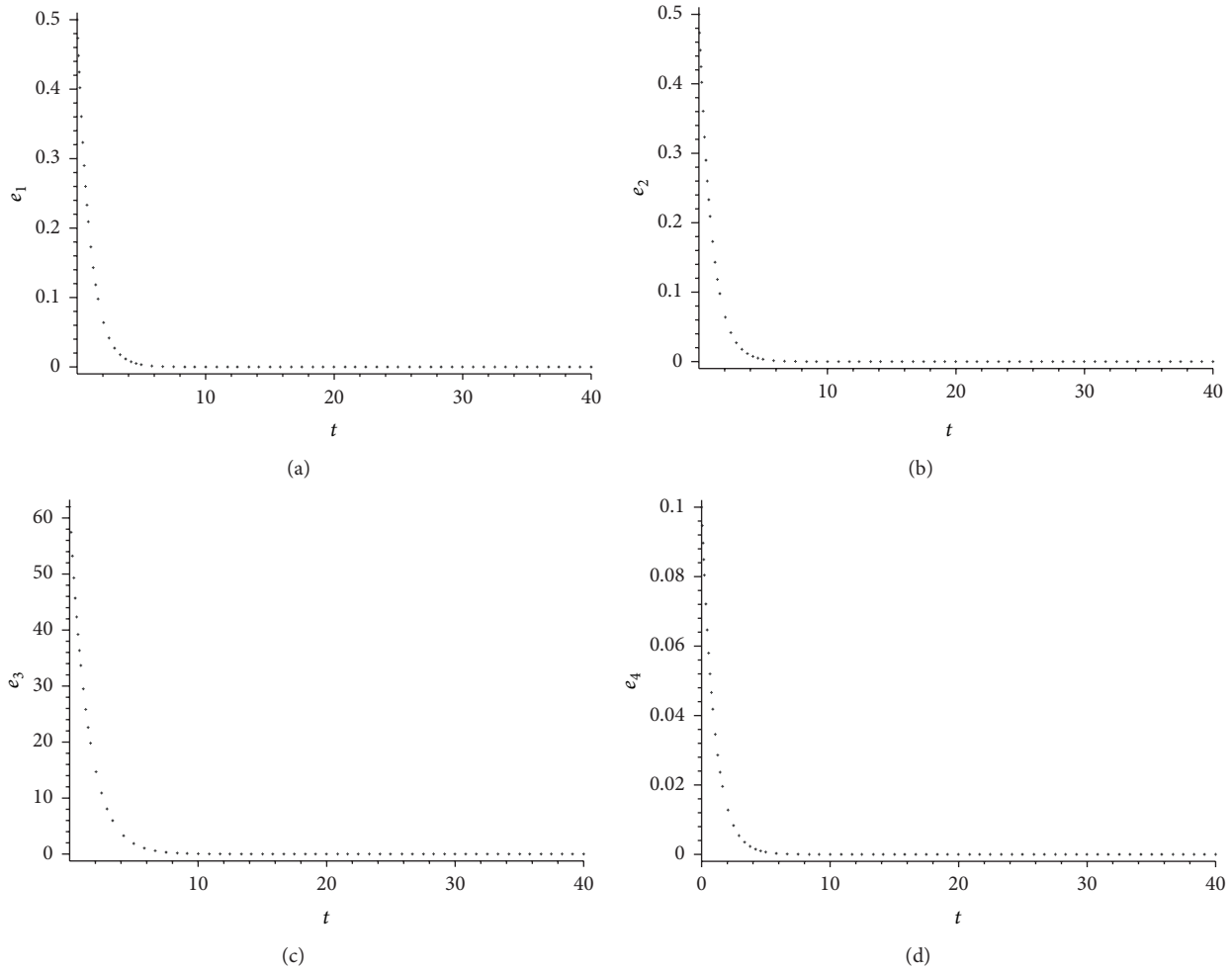$$+ (2ab - k_1 b - k_1 a + 2a - k_1 + b$$
$$+ d + a^2 - ca)\lambda^2$$

FIGURE 8: The dynamics of synchronization errors. (a) Signal e_1, (b) signal e_2, (c) signal e_3 and (d) signal e_4.

$$+ \left(-ca^2 - cab + 2ab + db + a^2 b - k_1 a\right.$$

$$+ a^2 - k_1 b - k_1 ba + d\right) \lambda$$

$$- ca^2 b - k_1 ba + a^2 b + db = 0. \tag{27}$$

Proposition 3. *If one chooses the control coefficients $k_1 = -30$, $m = 0.3$ and the parameters $a = 1.0$, $b = 0.7$, $c = 26$, and $d = 1.5$, the controlled chaotic Lorenz-Stenflo system* (9) *is asymptotically stable at the equilibrium* $(0, 0, 0, 0)$.

The proof of Proposition 3 is the same as Proposition 1, which is straightforward and thus is omitted.

In the following, we give the eigenvalues via the compute simulation. When the parameters were selected by the above value, we obtain the Jacobian matrix

$$J = \begin{pmatrix} -31.0 & 1.0 & 0 & 1.5 \\ 26 & -1 & 0 & 0 \\ 0 & 0 & -0.7 & 0 \\ -1.0 & 0 & 0 & -1.0 \end{pmatrix}. \tag{28}$$

The characteristic equation of J changes the following:

$$\lambda^4 + 33.7\lambda^3 + 61.60\lambda^2 + 33.450\lambda + 4.55 = 0. \tag{29}$$

The eigenvalues of the above equation are

$$\lambda_1 = -31.795569, \quad \lambda_2 = -0.20443,$$
$$\lambda_3 = -1, \quad \lambda_4 = -0.70000. \tag{30}$$

Thus the zero solution of system (9) is exponentially stable; Proposition 3 is proved.

Numerical simulations are used to investigate the controlled chaotic Lorenz-Stenflo system (25) using the fourth-order Runge-Kutta scheme with time step 0.01. The initial values are taken as $[x(0) = 1, y(0) = 0.7, z(0) = 20, w(0) = 0.1]$. The behaviors of the states (x, y, z, w) of the controlled chaotic Lorenz-Stenflo system (25) with time are displayed in Figures 5(a)–5(d).
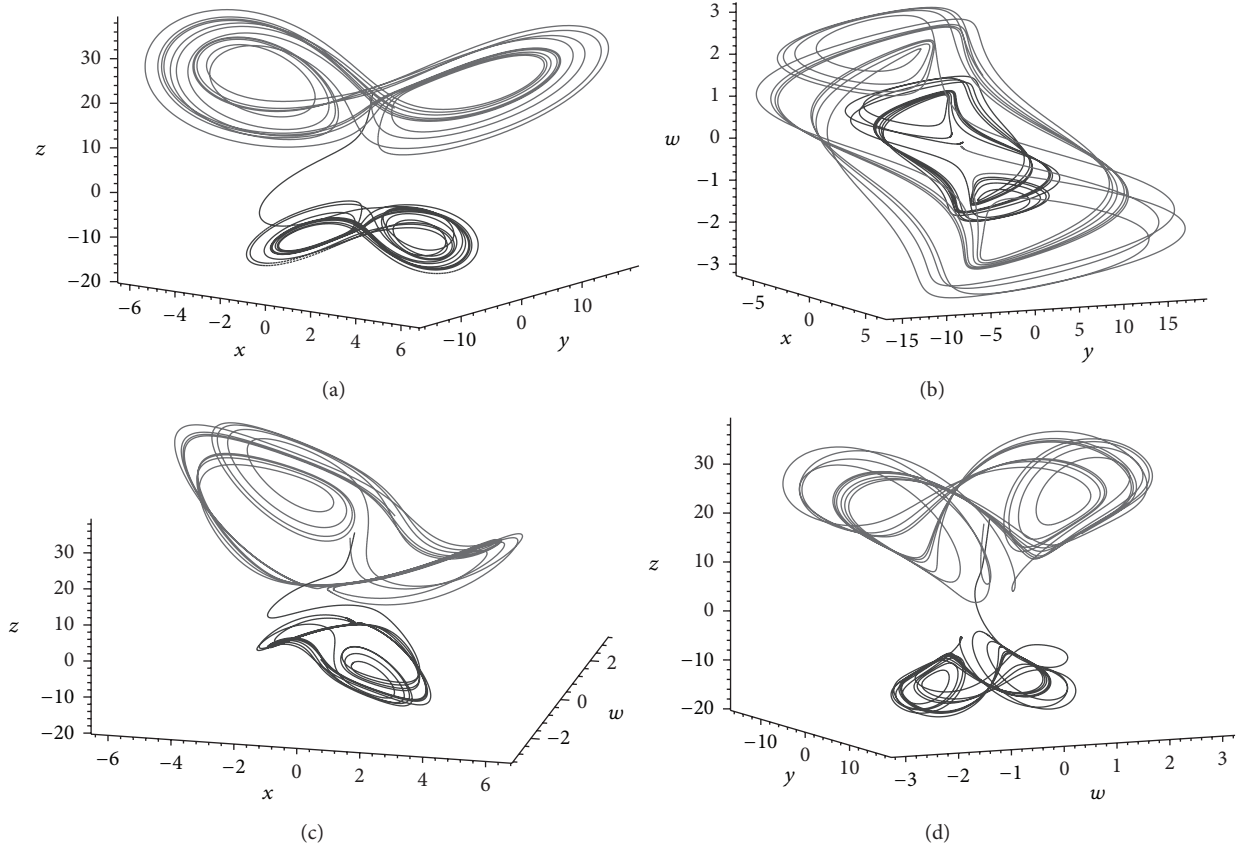
FIGURE 9: The projection of the synchronized attractors in different spaces: (a) (x, y, z), (b) (x, y, w), (c) (x, w, z), and (d) (y, w, z). The solid line denotes and the drive system; the dashed line denotes respond system synchronized.

4. Globally Exponential Hyperchaotic Projective Synchronization Control

Consider two chaotic systems given by

$$\dot{x}_m = f\left(x_m, t\right), \tag{31}$$

$$\dot{y}_s = g\left(y_s, t\right) + u\left(x_m, y_s, t\right), \tag{32}$$

where $x_m = (x_{1m}, x_{2m}, \ldots x_{nm})^T$, $y_s = (y_{1s}, y_{2s}, \ldots y_{ns})^T$, $f, g \in C^r[R_+ \times R^n, R^n]$, $u \in C^r[R_+ \times R^n \times R^n, R^n]$, and $r \geq 1$. R_+ comprises the set of non negative real numbers. Assume that (31) is the master system, (32) is the slave system, and $u(x_m, y_s, t)$ is the control vector. Let the error state be

$$e\left(t\right) = \left[e_1\left(t\right), e_2\left(t\right) \ldots, e_n\left(t\right)\right]^T$$

$$= \left[x_{1m} - \left(a_{11}y_{1s} + a_{12}\right)y_{1s}, \ldots, x_{nm} \right. \tag{33}$$

$$\left. - \left(a_{n1}y_{ns} + a_{n2}\right)y_{1s}\right].$$

Then the error dynamics of $e(t)$ are defined by

$$\dot{e}\left(t\right) = f\left(x_m, t\right) - g\left(y_s, t\right) - u\left(x_m, y_s, t\right). \tag{34}$$

The slave and master systems are said to be exponential, hyperchaotic, projective and synchronized if, for all $x_m(t_0)$, $y_s(t_0) \in R^n$, and $i \in R^n$, $\|x_m - (a_{i1}y_s + a_{i2})y_s\| \to 0$ as $t \to \infty$.

Lemma 4 (see [27, 28]). *The zero solution of the error dynamical system* (34) *is globally and exponentially stable; the master-slave systems* (31) *and* (32) *are globally and exponentially projective, synchronized, if there exists a positive definite quadratic polynomial* $V = (e_1, e_2, \ldots e_n)P(e_1, e_2, \ldots e_n)^T$ *such that* $dV/dt = (e_1, e_2, \ldots e_n)Q(e_1, e_2, \ldots e_n)^T$. *Moreover, the following negative Lyapunov exponent estimation for the error dynamical system* (34) *holds:*

$$\sum_{i=1}^{n} e_i^2\left(t\right) \leq \frac{\lambda_{\max}\left(P\right)}{\lambda_{\min}\left(P\right)} \sum_{i=1}^{n} e_i^2\left(0\right) \exp\left[-\frac{\lambda_{\max}\left(Q\right)}{\lambda_{\min}\left(P\right)}\left(t\right)\right], \tag{35}$$

where $P = P^T \in R^{n \times n}$ *and* $Q = Q^T \in R^{n \times n}$ *are both positive definite matrices,* $\lambda_{\max}(P)$ *and* $\lambda_{\min}(P)$ *stand for the minimum and maximum eigenvalues of the matrix P, respectively, and* $\lambda_{\min}(Q)$ *denotes the minimum eigenvalue of the matrix Q.*

In the following, we consider the hyperchaotic system (1) as a master system:

$$\begin{aligned}
\dot{x}_m &= a\left(y_m - x_m\right) + dw_m, \\
\dot{y}_m &= x_m\left(c - z_m\right) - y_m, \\
\dot{z}_m &= y_m x_m - bz_m, \\
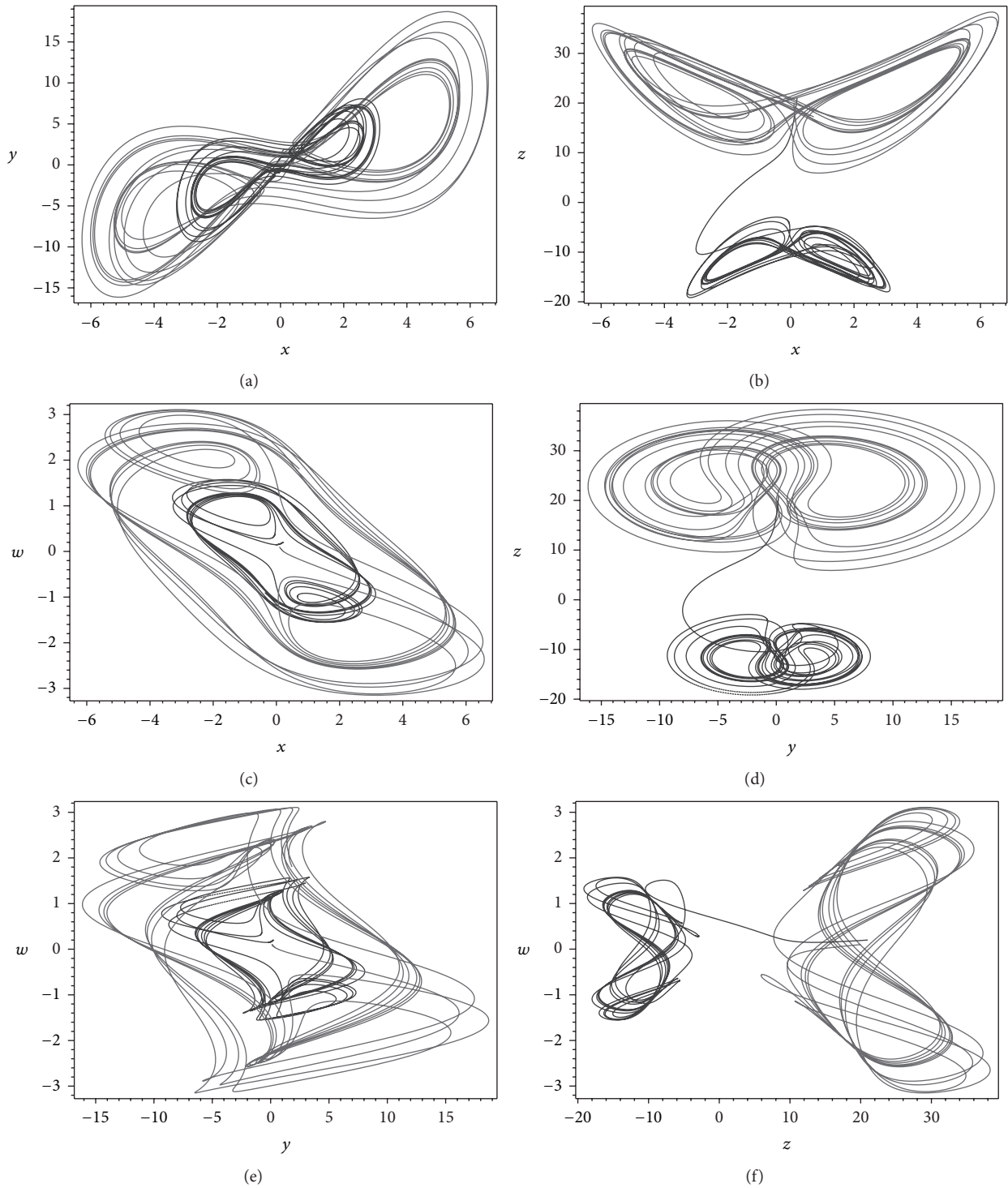\dot{w}_m &= -x_m - aw_m
\end{aligned} \tag{36}$$

Figure 10: Simulated phase portraits of the chaotic system (1), projected on (a) the x-y plane, (b) the x-z plane, (c) the x-w plane, (d) the y-z plane, (e) the y-w plane, and (f) the z-w plane.

and the system related to (36), given by

$$
\begin{aligned}
\dot{x}_s &= a\left(y_s - x_s\right) + dw_s + u_1, \\
\dot{y}_s &= x_s\left(c - z_s\right) - y_s + u_2, \\
\dot{z}_s &= y_s x_s - bz_s + u_3, \\
\dot{w}_s &= -x_s - aw_s + u_4,
\end{aligned}
\tag{37}
$$

as a slave system, where the subscripts "m" and "s" stand for the master system and slave system, respectively. Let the error state be

$$
\begin{aligned}
e(t) &= \left(e_1, e_2, e_3, e_4\right)^T \\
&= \left[x_m - \left(a_{11}x_s + a_{12}\right)x_s,\right.
\end{aligned}
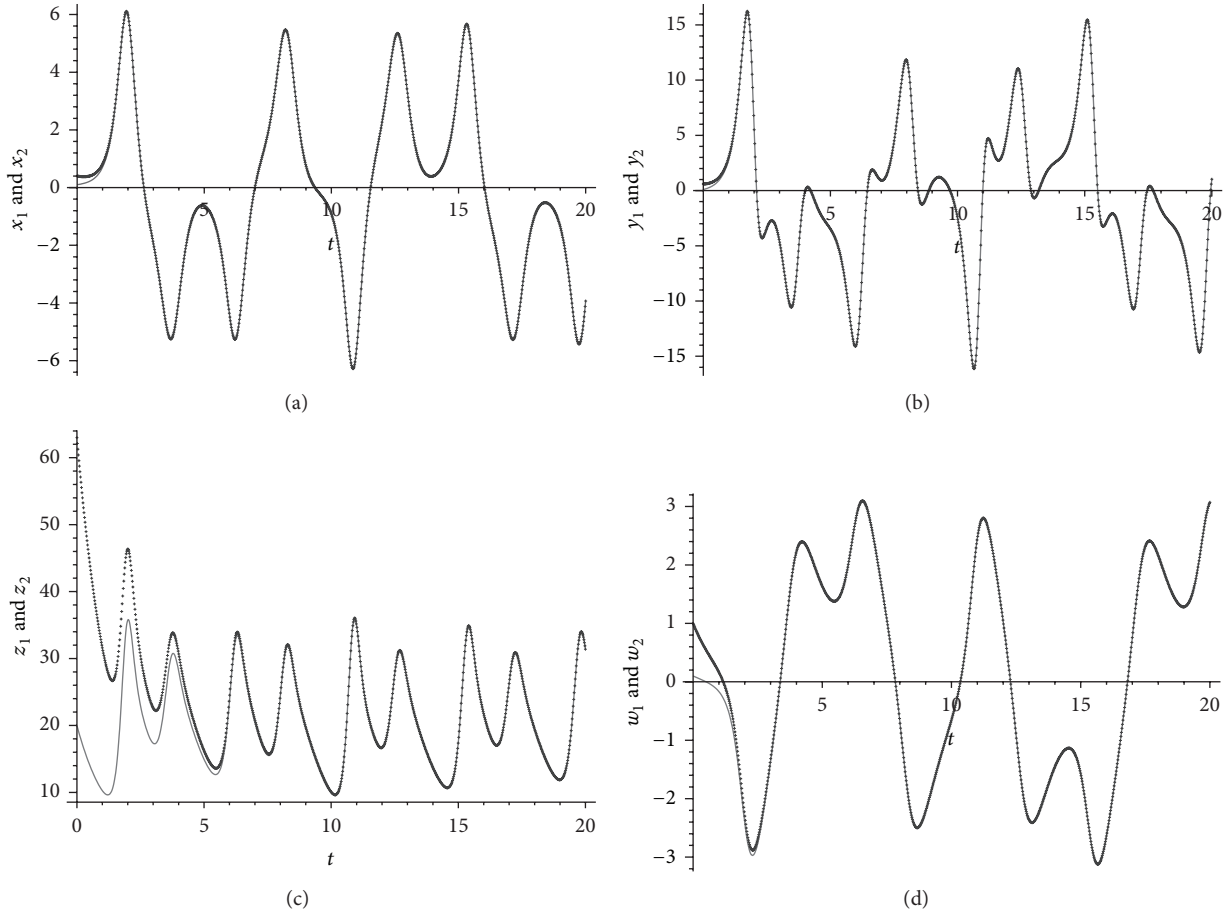$$

(a)

(b)

(c)

(d)

FIGURE 11: The solutions of the master and slave systems with control law. (a) Signals x_1 (the dashed line) and x_2 (the solid line). (b) Signals y_1 (the dashed line) and y_2 (the solid line). (c) Signals z_1 (the dashed line) and z_2 (the solid line). (d) Signals w_1 (the dashed line) and w_2 (the solid line).

$$
\begin{aligned}
& y_m - \left(a_{21} y_s + a_{22}\right) y_s, \\
& z_m - \left(a_{31} z_s + a_{32}\right) z_s, \\
& w_m - \left(a_{41} w_s + a_{42}\right) w_s \big]^T.
\end{aligned}
\tag{38}
$$

Then the derivative of $e(t)$ along the trajectories of (36) and (37), we obtain the error system:

$$
\begin{aligned}
\dot{e}_1 = & \, a\left(y_m - x_m\right) + dw_m - 2a_{11}x_s \\
& \times \left[a\left(y_s - x_s\right) + bw_s + u_1\right] \\
& - \left[a\left(y_s - x_s\right) + bw_s + u_1\right] a_{12}, \\
\dot{e}_2 = & \, \left(c - z_m\right) x_m - y_m - 2a_{21}y_s \\
& \times \left[\left(c - z_s\right) x_s - y_s + u_2\right] \\
& - \left[\left(c - z_s\right) x_s - y_s + u_2\right] a_{22}, \\
\dot{e}_3 = & -bz_m + x_m y_m - 2a_{31}z_s \\
& \times \left(-dz_s + x_s y_s + u_3\right) \\
& - \left(-dz_s + x_s y_s + u_3\right) a_{32},
\end{aligned}
$$

$$
\begin{aligned}
\dot{e}_4 = & -x_m - aw_m - 2a_{41}w_s\left(-x_s - aw_s + u_4\right) \\
& - \left(-x_s - aw_s + u_4\right) a_{42}.
\end{aligned}
\tag{39}
$$

To demonstrate the synchronization control between systems (36) and (37), we have the following cases based on [29–44].

Case 1 (modified projective synchronization control).

Theorem I. *When* $[a_{11}, a_{12}, a_{21}, a_{22}, a_{31}, a_{32}, a_{41}, a_{42}] = [0, m, 0, m, 0, m, 0, m]$, $a > 0$ *and* $b > 0$. *For the hyperchaotic system* (1), *if one of the following families of feedback controllers* u_i ($i = 1, 2, 3, 4$) *is given for the slave system* (36):

$$
\begin{aligned}
u_1 & = \frac{(d - b)\, mw_2 - v_1}{m}, \\
u_2 & = \frac{(1 - m)\, mx_2 z_2 - v_2}{m}, \\
u_3 & = \frac{\left(mx_2 y_2 - bz_2 + dz_2 - x_2 y_2\right) m - v_3}{m}, \\
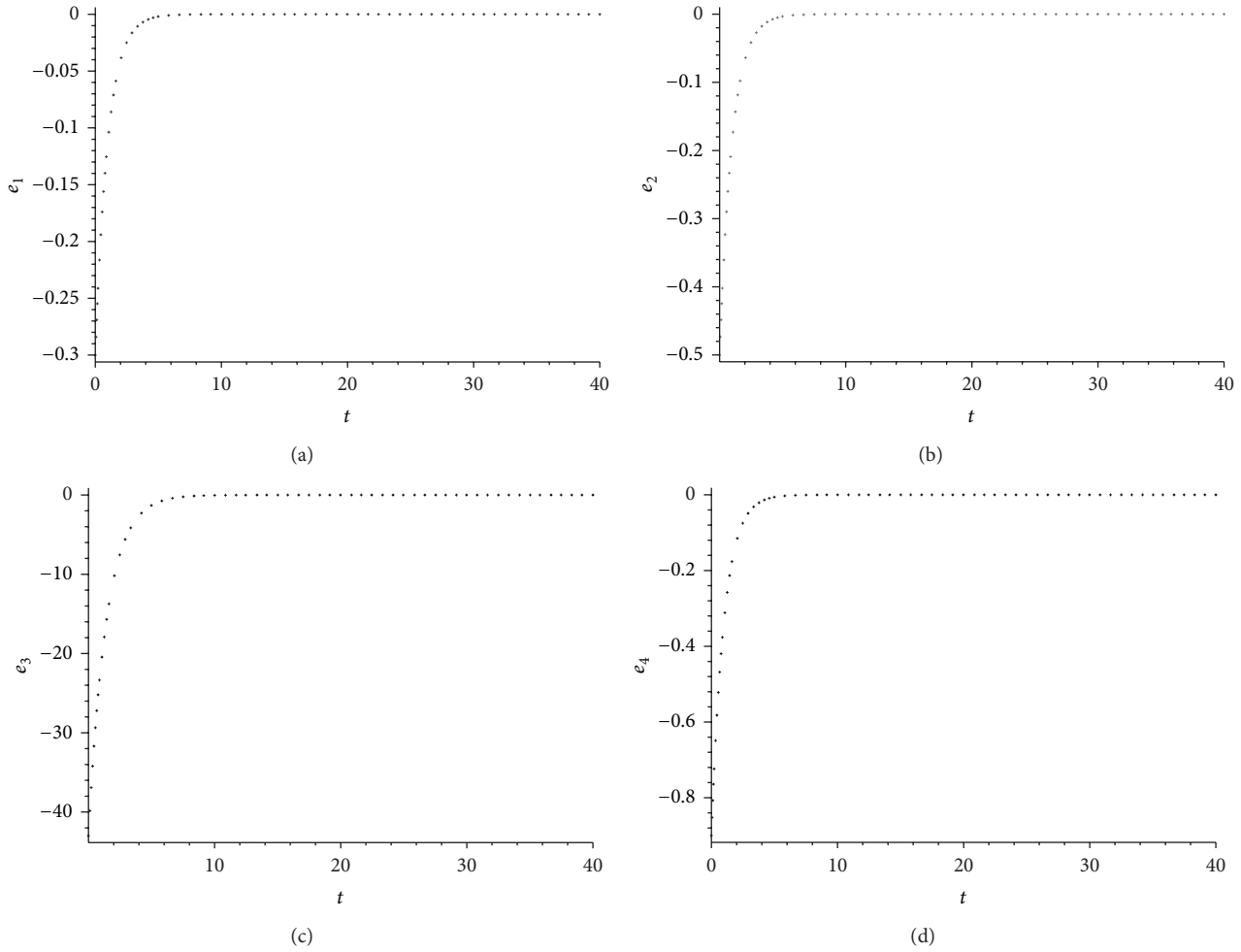u_4 & = \frac{-x_1 + mx_2 - v_4}{m},
\end{aligned}
\tag{40}
$$

FIGURE 12: The dynamics of synchronization errors. (a) Signal e_1, (b) signal e_2, (c) signal e_3, and (d) signal e_4.

there exist many possible choices for v_1, v_2, v_3, and v_4. Then the zero solution of the error dynamical system (39) *is globally and exponentially stable, and thus globally exponential modified projective synchronization can be achieved.*

The concrete proof of Theorem I can be demonstrated by Appendix B. In the following, tracking numerical simulations are used to solve differential equations (36), (37), and (42) with Runge-Kutta integration method. The initial values of the drive system and response system are $x_1(0) = 0.1$, $y_1(0) = 0.1$, $z_1(0) = 20$, and $w_1(0) = 0.1$ and $x_2(0) = 0.2$, $y_2(0) = 0.2$, $z_2(0) = 21$, and $w_2(0) = 0.2$ respectively. The parameters are chosen to be $m = -2$, $a = 1.0$, $b = 0.7$, $d = 1.5$, and $c = 26$ so that the Lorenz-Stenflo hyperchaotic system exhibits a chaotic behavior if no control is applied. The numerical simulation of the master and the slave systems without active synchronization control law is shown in Figures 6(a)–6(d). The diagram of the solutions of the master and the slave systems with feedback control law is presented in Figures 7(a)–7(d). The synchronization errors are shown in Figures 8(a)–8(d). Figures 9(a)–9(d) depicts the projection of the

synchronized attractors. Figures 10(a)–10(f) depicts the phase portraits of the synchronized attractors.

Case 2 (generalized projective synchronization control).

Theorem II. *When* $[a_{11}, a_{12}, a_{21}, a_{22}, a_{31}, a_{32}, a_{41}, a_{42}] = [0, m_1, 0, m_2, 0, m_3, 0, m_4]$, m_i's *are different,* $a > 0$ *and* $b > 0$. *For the hyperchaotic system* (1), *if one of the following families of feedback controllers* u_i ($i = 1, 2, 3, 4$) *is given for the slave system* (36)*:*

$$u_1 = \frac{(m_2 - m_1)\,ay_2 + (dm_4 - m_1 b)\,w_2 - v_1}{m_1},$$

$$u_2 = \frac{(m_1 - m_2)\,cx_2 + (m_2 - m_1 m_3)\,cx_2 - v_2}{m_2},$$

$$u_3 = \frac{(d - b)\,m_3 z_2 + (m_1 m_2 - m_3)\,cx_2 - v_3}{m_3},$$
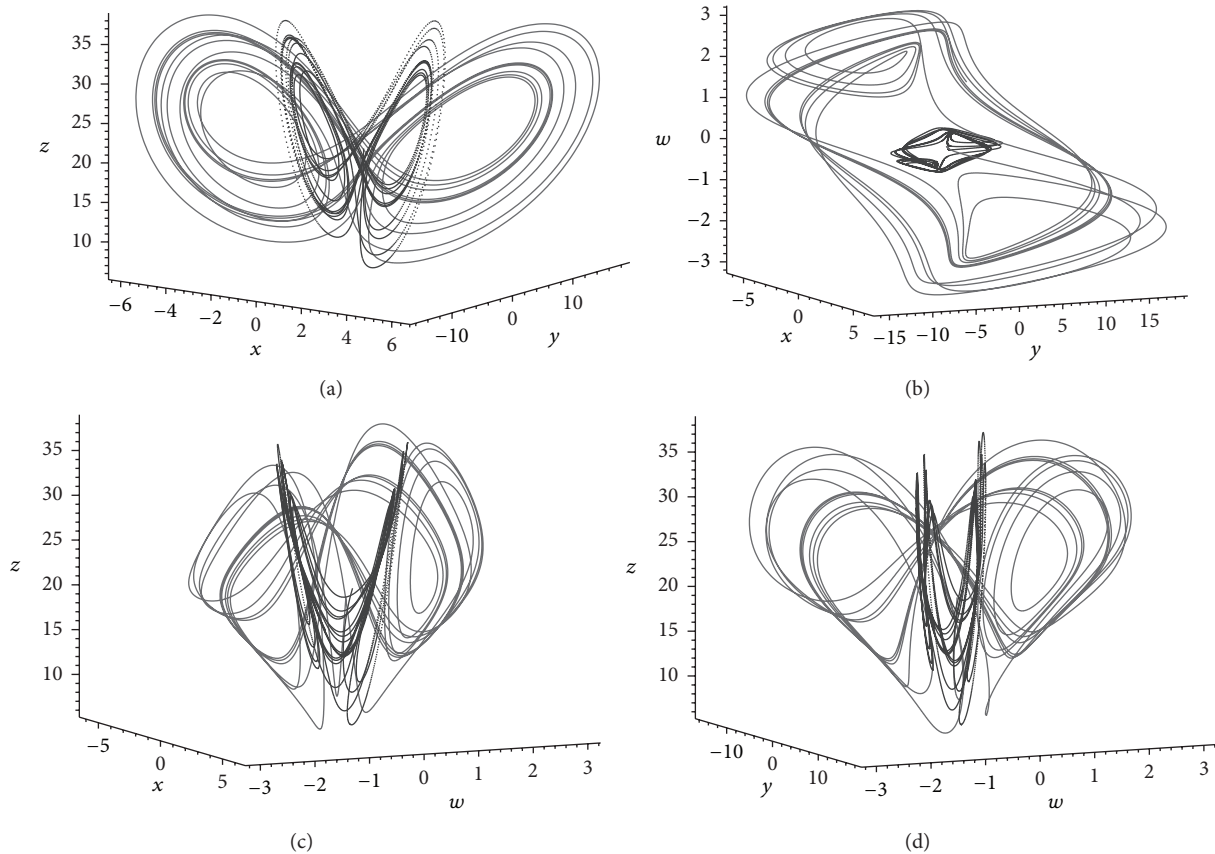
$$u_4 = \frac{-x_1 + m_4 x_2 - v_4}{m_4},$$

(41)

FIGURE 13: The function projection of the synchronized attractors in different spaces: (a) (x, y, z), (b) (x, y, w), (c) (x, w, z), and (d) (y, w, z). The solid line denotes the drive system; the dashed line denotes respond system synchronized.

there exist many possible choices for v_1, v_2, v_3, *and* v_4. *Then the zero solution of the error dynamical system* (39) *is globally and exponentially stable, and thus globally exponential generalized projective synchronization.*

The concrete proof of Theorem II can be demonstrated by Appendix B. In the following, tracking numerical simulations are used to solve differential equations (36), (37), and (39) with Runge-Kutta integration method. The parameters are chosen to be $m_1 = 2$, $m_2 = 3$, $m_3 = 3$, and $m_4 = 5$. The initial values and others parameters are the same as the above cases so that the Lorenz-Stenflo hyperchaotic system exhibits a chaotic behavior if no control is applied. The diagram of the solutions of the master and the slave systems with feedback control law is presented in Figures 11(a)–11(d). The synchronization errors are shown in Figures 12(a)–12(d).

Case 3 (function synchronization control [45–58]).

Theorem III. *When* $f_1 = a_{11}x_2 + a_{12}$, $f_2 = a_{21}y_2 + a_{22}$, $f_3 = a_{31}z_2 + a_{32}$, $f_4 = a_{41}w_2 + a_{42}$, $a_{i1} \neq 0$, $a > 0$, $b > 0$. *For the hyperchaotic system* (1), *if one of the following families of feedback controllers* u_i ($i = 1, 2, 3, 4$) *is given for the slave system* (36):

$$u_1 = \frac{(f_2 - f_1)\,ay_2 + (df_4 - f_1 b)\,w_2 - k_1 e_1}{f_1},$$

$$u_2 = \frac{(f_1 - f_2)\,cx_2 + (f_2 - f_1 f_3)\,cx_2 - k_2 e_2}{f_2},$$

$$u_3 = \frac{(d - b)\,f_3 z_2 + (f_1 f_2 - f_3)\,cx_2 - k_3 e_3}{f_3},$$ (42)

$$u_4 = \frac{-x_1 + f_4 x_2 - k_4 e_4}{f_4},$$

where $k_1 > 0$, $k_2 > 0$, $k_3 > 0$, *and* $k_4 > 0$, *then the zero solution of the error dynamical system* (39) *is globally stable, and thus global function, projective synchronization occurs between the master systems* (36) *and* (37).

The concrete Proof of Theorem III can be demonstrated by Appendix B. In the following, tracking numerical simulations are used to solve differential equations (36), (37), and (39) with Runge-Kutta integration method. The initial values and the parameters are the same as the above cases so that the Lorenz-Stenflo hyperchaotic system exhibits a chaotic behavior if no control is applied. The diagram of the solutions
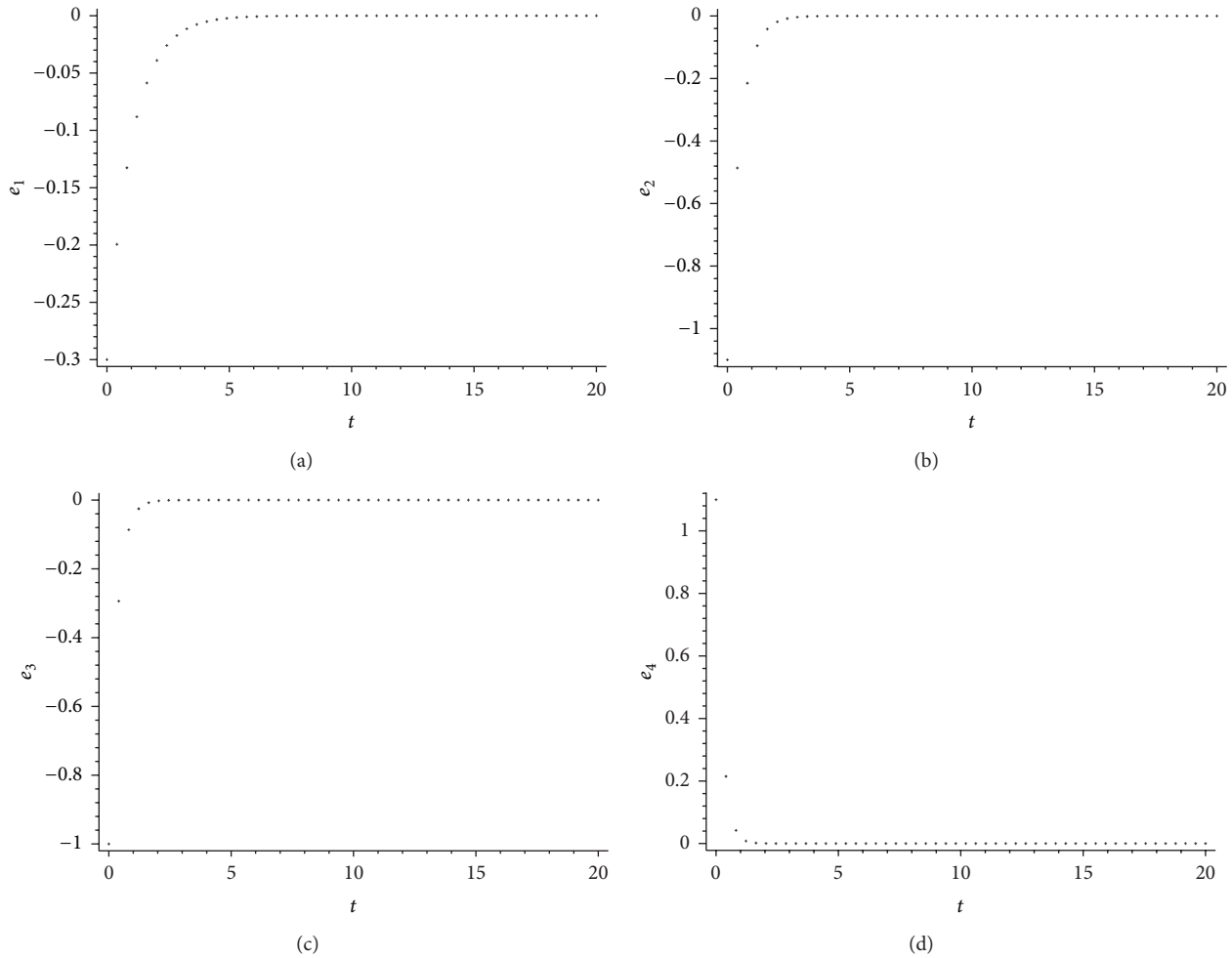
(a)

(b)

(c)

(d)

FIGURE 14: The dynamics of synchronization errors. (a) Signal e_1, (b) signal e_2, (c) signal e_3 and (d) signal e_4.

of the master and the slave systems with active control law is presented in Figures 13(a)–13(d). The synchronization errors are shown in Figures 14(a)–14(d).

5. Summary and Conclusions

In this paper, we have introduced the tracking control and generalized synchronization of the hyperchaotic system which is different from the Lorenz-Stenflo attractor. We suppress the chaos to unstabilize equilibrium via three feedback methods, and we achieve three globally generalized synchronization controls of two Lorenz-Stenflo systems. As a result, some powerful controllers are obtained. Then, we investigate the hyperchaotic system applying the complex system calculus technique. Moreover, numerical simulations are used to verify the effectiveness of our results, through the contrast between the orbits before being stabilized and the ones after being stabilized.

Appendices

A. The Maple Program

> *restart: with(student): with(PDEtools): with(linalg): with (LinearAlgebra)*:

> $J := matrix(4, 4, [[A, a, 0, d], [c, B, 0, 0], [0, 0, C, 0], [-1, 0, 0, D]])$;

> $U := charmat(J, \lambda)$;

> $poly1 := collect(det(U), \lambda)$;

> $a1 := coeff(poly1, \lambda, 3)$;

> $a2 := coeff(poly1, \lambda, 2)$;

> $a3 := coeff(poly1, \lambda, 1)$;

> $a4 := coeff(poly1, \lambda, 0)$;

> $H := matrix(4, 4, [a1, a3, 0, 0, 1, a2, a4, 0, 0, a1, a3, 0, 0, 1, a2, a4])$;

> $H11 := submatrix(H, 1..1, 1..1)$;

> $H22 := submatrix(H, 1..2, 1..2);$

> $H33 := submatrix(H, 1..3, 1..3);$

> $H44 := submatrix(H, 1..4, 1..4);$

> $H1 := det(H11);$

> $H2 := det(H22);$

> $H3 := det(H33);$

> $H4 := det(H44).$

B. The Proof of Theorem

Proof of Theorem I. Consider the controller (40) and choose the following v_i:

$$v_1 = -ae_2 - de_4,$$
$$v_2 = -ce_1 + e_1e_3 + e_1mz_2 + mx_2e_3,$$
$$v_3 = -e_2e_1 - e_2mx_2 - my_2e_1,$$
$$v_4 = (a - 1)e_4.$$

(B.1)

Then the system (39) is reduced into

$$\dot{e}_1 = -ae_1,$$
$$\dot{e}_2 = -e_2,$$
$$\dot{e}_3 = -be_3,$$
$$\dot{e}_4 = -e_4.$$

(B.2)

Let us consider the Lyapunov function for the system (B.2) as follows:

$$V(e_1, e_2, e_3, e_4) = \frac{1}{2}\left(e_1^2 + e_2^2 + e_3^2 + e_4^2\right).$$

(B.3)

In addition, the derivative of V has the form

$$\frac{dV(t)}{dt} = -\left(ae_1^2 + e_2^2 + be_3^2 + e_4^2\right),$$

(B.4)

which is negatively defined. So (B.2) is asymptotically stable. This implies that the two Lorenz-Stenflo hyperchaotic systems are projective and synchronized. □

Proof of Theorem II. Consider the controller (41) and choose v_i as follows:

$$v_1 = -ae_2 - de_4,$$
$$v_2 = -ce_1 + e_1e_3 + e_1m_3z_2 + m_1x_2e_3,$$
$$v_3 = -e_2e_1 - e_2m_1x_2 - m_2y_2e_1,$$
$$v_4 = (a - 1)e_4.$$

(B.5)

Then the following steps are the same (B.2), (B.3), and (B.4). So we know that the two Lorenz-Stenflo hyperchaotic systems are modified, projective, and synchronized. □

Proof of Theorem III. Consider the controller (42) and choose the following positive definite, quadratic form of Lyapunov function:

$$V(t) = \frac{1}{2}\left[e_1^2 + e_2^2 + e_3^2 + e_4^2\right].$$

(B.6)

We differentiate $V(t)$ and substitute the trajectory of system (39) which yields

$$\left.\frac{dV(t)}{dt}\right|_{(18)} = e_1\dot{e}_1 + e_2\dot{e}_2 + e_3\dot{e}_3$$
$$= -k_1e_1^2 - k_2e_2^2 - k_3e_3^2 - k_4e_4^2$$
$$= -[e_1, e_2, e_3, e_4] P[e_1, e_2, e_3, e_4]^T,$$

(B.7)

where $P = \text{diag}(k_1, k_2, k_3, k_4)$, which implies that the conclusion of Theorem III is true. So (39) is asymptotically stable. This implies that the two Lorenz-Stenflo hyperchaotic systems are projective synchronized functions. □

References

[1] G. Chen and X. Dong, *From Chaos to Order*, vol. 24, World Scientific, Singapore, 1998.

[2] S. Boccaletti, J. Kurths, G. Osipov, D. L. Valladares, and C. S. Zhou, "The synchronization of chaotic systems," *Physics Reports*, vol. 366, no. 1-2, pp. 1–101, 2002.

[3] L. M. Pecora and T. L. Carroll, "Synchronization in chaotic systems," *Physical Review Letters*, vol. 64, no. 8, pp. 821–824, 1990.

[4] O. E. Rössler, "Continuous chaos-four prototype equations," *Annals of the New York Academy of Sciences*, vol. 316, pp. 376–392, 1979.

[5] M. T. Yassen, "Synchronization hyperchaos of hyperchaotic systems," *Chaos, Solitons and Fractals*, vol. 37, no. 2, pp. 465–475, 2008.

[6] X. Liao and P. Yu, "Analysis on the globally exponent synchronization of Chua's circuit using absolute stability theory," *International Journal of Bifurcation and Chaos in Applied Sciences and Engineering*, vol. 15, no. 12, pp. 3867–3881, 2005.

[7] Y. Li, W. K. S. Tang, and G. Chen, "Generating hyperchaos via state feedback control," *International Journal of Bifurcation and Chaos in Applied Sciences and Engineering*, vol. 15, no. 10, pp. 3367–3375, 2005.

[8] Z. Yan, "Controlling hyperchaos in the new hyperchaotic Chen system," *Applied Mathematics and Computation*, vol. 168, no. 2, pp. 1239–1250, 2005.

[9] M. Boutayeb, M. Darouach, and H. Rafaralahy, "Generalized state-space observers for chaotic synchronization and secure communication," *IEEE Transactions on Circuits and Systems*, vol. 49, no. 3, pp. 345–349, 2002.

[10] X. P. Guan, Z. P. Fan, and C. L. Chen, *Chaos Control and Its Application in Secure Communication*, National Defence Industry Press, Beijing, China, 2002.

[11] S. Sundar and A. A. Minai, "Synchronization of randomly multiplexed chaotic systems with application to communication," *Physical Review Letters*, vol. 85, no. 25, pp. 5456–5459, 2000.

[12] M. Feki, "An adaptive chaos synchronization scheme applied to secure communication," *Chaos, Solitons and Fractals*, vol. 18, no. 1, pp. 141–148, 2003.

[13] Z. Yan, "Q-S synchronization in 3D Henon-like map and generalized Henon map via a scalar controller," *Physics Letters A*, vol. 342, pp. 309–317, 2005.

[14] Z. Yan, "Q-S (lag or anticipated) synchronization backstepping scheme in a class of continuous-time hyperchaotic systems—a symbolic-numeric computation approach," *Chaos*, vol. 15, no. 2, pp. 023902–023909, 2005.

[15] M.-C. Ho, Y.-C. Hung, and C.-H. Chou, "Phase and anti-phase synchronization of two chaotic systems by using active control," *Physics Letters A*, vol. 296, no. 1, pp. 43–48, 2002.

[16] L. Pan, W. Zhou, J. Fang, and D. Li, "A novel active pinning control for synchronization and anti-synchronization of new uncertain unified chaotic systems," *Nonlinear Dynamics*, vol. 62, no. 1-2, pp. 417–425, 2010.

[17] H. Salarieh and A. Alasty, "Adaptive synchronization of two chaotic systems with stochastic unknown parameters," *Communications in Nonlinear Science and Numerical Simulation*, vol. 14, no. 2, pp. 508–519, 2009.

[18] M. Hu and Z. Xu, "Adaptive feedback controller for projective synchronization," *Nonlinear Analysis. Real World Applications*, vol. 9, no. 3, pp. 1253–1260, 2008.

[19] Y.-J. Liu, W. Wang, S.-C. Tong, and Y.-S. Liu, "Robust adaptive tracking control for nonlinear systems based on bounds of fuzzy approximation parameters," *IEEE Transactions on Systems, Man, and Cybernetics A*, vol. 40, no. 1, pp. 170–184, 2010.

[20] Y.-J. Liu and Y.-Q. Zheng, "Adaptive robust fuzzy control for a class of uncertain chaotic systems," *Nonlinear Dynamics*, vol. 57, no. 3, pp. 431–439, 2009.

[21] Y.-J. Liu and W. Wang, "Adaptive fuzzy control for a class of uncertain nonaffine nonlinear systems," *Information Sciences*, vol. 177, no. 18, pp. 3901–3917, 2007.

[22] E. M. Elabbasy, H. N. Agiza, and M. M. El-Dessoky, "Adaptive synchronization of a hyperchaotic system with uncertain parameter," *Chaos, Solitons & Fractals*, vol. 30, no. 5, pp. 1133–1142, 2006.

[23] J. Huang, "Adaptive synchronization between different hyperchaotic systems with fully uncertain parameters," *Physics Letters A*, vol. 372, no. 27-28, pp. 4799–4804, 2008.

[24] Y.-J. Liu, S.-C. Tong, W. Wang, and Y.-M. Li, "Observer-based direct adaptive fuzzy control of uncertain nonlinear systems and its applications," *International Journal of Control, Automation and Systems*, vol. 7, no. 4, pp. 681–690, 2009.

[25] C. Li, X. Liao, and K.-w. Wong, "Lag synchronization of hyperchaos with application to secure communications," *Chaos, Solitons & Fractals*, vol. 23, no. 1, pp. 183–193, 2005.

[26] L. Stenflo, "Generalized Lorenz equations for acoustic-gravity waves in the atmosphere," *Physica Scripta*, vol. 53, no. 1, pp. 83–84, 1996.

[27] Z. Yan and P. Yu, "Linear feedback control, adaptive feedback control and their combination for chaos (lag) synchronization of LC chaotic systems," *Chaos, Solitons and Fractals*, vol. 33, no. 2, pp. 419–435, 2007.

[28] X. Liao and P. Yu, "Study of globally exponential synchronization for the family of Rössler systems," *International Journal of Bifurcation and Chaos in Applied Sciences and Engineering*, vol. 16, no. 8, pp. 2395–2406, 2006.

[29] D. Ghosh and S. Bhattacharya, "Projective synchronization of new hyperchaotic system with fully unknown parameters," *Nonlinear Dynamics*, vol. 61, no. 1-2, pp. 11–21, 2010.

[30] D.-Z. Ma, H.-G. Zhang, Z.-S. Wang, and J. Feng, "Fault tolerant synchronization of chaotic systems based on T-S fuzzy model with fuzzy sampled-data controller," *Chinese Physics B*, vol. 19, no. 5, Article ID 050506, 2010.

[31] S. S. Yang and C. K. Duan, "Generalized synchronization in chaotic systems," *Chaos, Solitons and Fractals*, vol. 9, no. 10, pp. 1703–1707, 1998.

[32] Y.-W. Wang and Z.-H. Guan, "Generalized synchronization of continuous chaotic system," *Chaos, Solitons and Fractals*, vol. 27, no. 1, pp. 97–101, 2006.

[33] M. G. Rosenblum, A. S. Pikovsky, and J. Kurths, "Phase synchronization of chaotic oscillators," *Physical Review Letters*, vol. 76, no. 11, pp. 1804–1807, 1996.

[34] Y. Zhang and J. Sun, "Chaotic synchronization and anti-synchronization based on suitable separation," *Physics Letters A*, vol. 330, no. 6, pp. 442–447, 2004.

[35] R. Aguilar-López and R. Martínez-Guerra, "Synchronization of a class of chaotic signals via robust observer design," *Chaos, Solitons and Fractals*, vol. 37, no. 2, pp. 581–587, 2008.

[36] J.-H. Chen, "Controlling chaos and chaotification in the Chen-Lee system by multiple time delays," *Chaos, Solitons and Fractals*, vol. 36, no. 4, pp. 843–852, 2008.

[37] H.-T. Yau and C.-S. Shieh, "Chaos synchronization using fuzzy logic controller," *Nonlinear Analysis. Real World Applications*, vol. 9, no. 4, pp. 1800–1810, 2008.

[38] Y. Li, Y. Chen, and B. Li, "Adaptive control and function projective synchronization in 2d discrete-time chaotic systems," *Communications in Theoretical Physics*, vol. 51, no. 2, pp. 270–278, 2009.

[39] Y. Li, Y. Chen, and B. Li, "Adaptive function projective synchronization of discrete-time chaotic systems," *Chiese Physics Letter*, vol. 26, pp. 040504–040509, 2009.

[40] Y. Li, B. Li, and Y. Chen, "Anticipated function synchronization with unknown parameters of discrete-time chaotic systems," *International Journal of Modern Physics C*, vol. 20, no. 4, pp. 597–608, 2009.

[41] Y. Li and B. Li, "Chaos control and projective synchronization of a chaotic Chen-Lee system," *Chinese Journal of Physics*, vol. 47, no. 3, pp. 261–270, 2009.

[42] J. Lü, X. Yu, G. Chen, and D. Cheng, "Characterizing the synchronizability of small-world dynamical networks," *IEEE Transactions on Circuits and Systems I*, vol. 51, no. 4, pp. 787–796, 2004.

[43] J. Lü, X. Yu, and G. Chen, "Chaos synchronization of general complex dynamical networks," *Physica A*, vol. 334, no. 1-2, pp. 281–302, 2004.

[44] J. Lü and G. Chen, "A time-varying complex dynamical network model and its controlled synchronization criteria," *Institute of Electrical and Electronics Engineers. Transactions on Automatic Control*, vol. 50, no. 6, pp. 841–846, 2005.

[45] X. Tang, J. Lu, and W. Zhang, "The FPS of chaotic system using backstepping design," *China Journal of Dynamics and Control*, vol. 5, pp. 216–219, 2007.

[46] Y. Chen and X. Li, "Function projective synchronization between two identical chaotic systems," *International Journal of Modern Physics C*, vol. 18, no. 5, pp. 883–888, 2007.

[47] H. Du, Q. Zeng, C. Wang, and M. Ling, "Function projective synchronization in coupled chaotic systems," *Nonlinear Analysis. Real World Applications*, vol. 11, no. 2, pp. 705–712, 2010.

[48] X.-J. Wu, H. Wang, and H.-T. Lu, "Hyperchaotic secure communication via generalized function projective synchronization," *Nonlinear Analysis. Real World Applications*, vol. 12, no. 2, pp. 1288–1299, 2011.

[49] H. Du, Q. Zeng, and C. Wang, "A General method for function projective synchronization," *International Journal of Innovative Computing, Information and Control*, vol. 5, no. 8, pp. 2239–2248, 2009.

[50] H. Du, Q. Zeng, and C. Wang, "Function projective synchronization of different chaotic systems with uncertain parameters," *Physics Letters A*, vol. 372, no. 33, pp. 5402–5410, 2008.

[51] Z. Wu and X. Fu, "Adaptive function projective synchronization of discrete chaotic systems with unknown parameters," *Chinese Physics Letters*, vol. 27, Article ID 050502, 2010.

[52] H. Du, F. Li, and G. Meng, "Robust function projective synchronization of two different chaotic systems with unknown parameters," *Journal of the Franklin Instituts*, vol. 348, no. 10, pp. 2782–2794, 2011.

[53] J. H. Park, "Further results on functional projective synchronization of genesiotesi chaotic system," *Modern Physics Letters B*, vol. 23, no. 15, pp. 1889–1895, 2009.

[54] R. Zhang, Y. Yang, Z. Xu, and M. Hu, "Function projective synchronization in drive-response dynamical network," *Physics Letters A*, vol. 374, no. 30, pp. 3025–3028, 2010.

[55] H. An and Y. Chen, "The function cascade synchronization method and applications," *Communications in Nonlinear Science and Numerical Simulation*, vol. 13, no. 10, pp. 2246–2255, 2008.

[56] Y. Chen, H. An, and Z. Li, "The function cascade synchronization approach with uncertain parameters or not for hyperchaotic systems," *Applied Mathematics and Computation*, vol. 197, no. 1, pp. 96–110, 2008.

[57] D.-J. Li, "Adaptive output feedback control of uncertain nonlinear chaotic systems based on dynamic surface control technique," *Nonlinear Dynamics. An International Journal of Nonlinear Dynamics and Chaos in Engineering Systems*, vol. 68, no. 1-2, pp. 235–243, 2012.

[58] Y. Li and C.-l. Zheng, "The complex network synchronization via chaos control nodes," *Journal of Applied Mathematics*, Article ID 823863, 11 pages, 2013.